

# Hafnium diboride thin films by chemical vapor deposition from a single source precursor

Sreenivas Jayaraman and Yu Yang

*Department of Materials Science and Engineering, University of Illinois at Urbana Champaign, 1304 West Green Street, Urbana, Illinois 61801 and Frederick Seitz Materials Research Laboratory, 104 South Goodwin Avenue, Urbana, Illinois 61801*

Do Young Kim and Gregory S. Girolami

*Department of Chemistry, University of Illinois at Urbana Champaign, 600 South Mathews Avenue, Urbana, Illinois 61801 and Frederick Seitz Materials Research Laboratory, 104 South Goodwin Avenue, Urbana, Illinois 61801*

John R. Abelson

*Department of Materials Science and Engineering, University of Illinois at Urbana Champaign, 1304 West Green Street, Urbana, Illinois 61801 and Frederick Seitz Materials Research Laboratory, 104 South Goodwin Avenue, Urbana, Illinois 61801*

(Received 26 April 2005; accepted 1 August 2005; published 24 October 2005)

High quality, stoichiometric thin films of hafnium diboride are deposited by chemical vapor deposition from the precursor  $\text{Hf}[\text{BH}_4]_4$  at deposition temperatures as low as 200 °C. An activation energy of 0.43 eV (41 kJ/mol) is obtained for the overall process as monitored by temperature programmed reaction studies. Films deposited at low temperatures (<500 °C) are structurally amorphous to x-ray diffraction; a 12 nm thick film is sufficient to prevent copper diffusion into silicon during a 600 °C anneal for 30 min. Films deposited above 500 °C are crystalline, but have a columnar microstructure with low density. All the films are metallic, but the low temperature amorphous films have the lowest resistivity  $\sim 440 \mu\Omega \text{ cm}$ . The process is also highly conformal, e.g., a 65 nm wide trench with a 19:1 depth-width aspect ratio was coated uniformly. © 2005 American Vacuum Society. [DOI: 10.1116/1.2049307]

## I. INTRODUCTION

Hafnium diboride is a metallic-ceramic material with attractive properties for microelectronic, hard coating, and other applications: it has a melting temperature of 3250 °C, a bulk resistivity of  $15 \mu\Omega \text{ cm}$ ,<sup>1,2</sup> and a bulk hardness of 29 GPa.<sup>1</sup> The related transition metal diborides  $\text{ZrB}_2$  and  $\text{TiB}_2$  have comparable properties and perform well as copper diffusion barriers for microelectronics;<sup>3–6</sup> they also have good corrosion resistance, e.g.,  $\text{ZrB}_2$  is resistant to molten zinc and aluminum.<sup>7</sup>  $\text{ZrB}_2$  thin films have been grown epitaxially on Si(111) substrates and used as templates (buffer layers) for the epitaxial overgrowth of GaN and AlGaN films.<sup>8–10</sup> All of the transition metal diborides have a hexagonal crystal structure. There is a 0.6% mismatch between the in-plane lattice constants of GaN and  $\text{ZrB}_2$ ; the mismatch between GaN and  $\text{HfB}_2$  is comparable at 1.4%, suggesting that  $\text{HfB}_2$  could also serve as a buffer layer on Si(111) substrates.

Despite these favorable properties, there has been relatively little use of transition metal diboride thin films in technological applications. The properties of transition metal diborides can degrade sharply when the composition is nonstoichiometric.<sup>11,12</sup> This phenomenon is consistent with the narrow compositional range for  $\text{MB}_2$  alloys in equilibrium phase diagrams, which implies that nonstoichiometric films will tend to phase segregate.<sup>13</sup> (By comparison, the phase field for TiN is several percent wide, which allows off-stoichiometric films to retain useful properties. Also, ex-

cess nitrogen on the growth surface can presumably be released as molecular  $\text{N}_2$ .) In physical vapor deposition techniques such as sputtering, there is no mechanism available to remove a nonstoichiometric excess of metal or boron atoms from the growth surface; resputtering may be introduced, but this mechanism does not intrinsically drive the film towards the desired  $\text{MB}_2$  composition. Thus, very precise control over the incident flux ratio must be maintained, which is difficult due to differences in the target angular emission and gas scattering effects for M and B atoms, convoluted over the reactor geometry. Nonetheless, magnetron sputtering has been used to obtain good  $\text{TiB}_2$ ,  $\text{ZrB}_2$ , and  $\text{CrB}_2$  coatings<sup>14–18</sup> and sputtered  $\text{HfB}_2$  has been used as the resistive heating element in ink-jet printers.<sup>19</sup>

Chemical vapor deposition (CVD) can afford stoichiometric  $\text{MB}_2$  films if the surface reactions during growth remove excess atoms as volatile by-products. Several CVD studies have used halogen-based precursors,<sup>20–22</sup> but the incorporation of residual halogen atoms has proven to be detrimental to film properties.<sup>23,24</sup> The single source precursor tetrakis(tetrahydroborato)hafnium,  $\text{Hf}[\text{BH}_4]_4$ , and its zirconium analog  $\text{Zr}[\text{BH}_4]_4$ , were reported as viable CVD precursors in 1988, but the growth kinetics were not studied in detail.<sup>25,26</sup> These molecules contain only the transition metal, boron, and hydrogen atoms, and thus obviate any complications associated with organic or halogen species. The idealized growth reaction for  $\text{HfB}_2$  is  $\text{Hf}[\text{BH}_4]_4(\text{g}) \rightarrow \text{HfB}_2(\text{s}) + \text{B}_2\text{H}_6(\text{g}) + 5\text{H}_2(\text{g})$ ; the reaction for  $\text{ZrB}_2$  is analogous.

Hf[BH<sub>4</sub>]<sub>4</sub> has also been used in a plasma-enhanced CVD process to make hard coatings, however, the films were overstoichiometric in boron.<sup>27</sup> We attribute the latter to the extensive precracking of the precursor by the plasma, such that surface reactions were unable to form volatile boron-containing species at a sufficient rate. This conclusion is plausible in view of the entropic demands in forming B<sub>2</sub>H<sub>6</sub> from small fragments.

In this work, we deposit HfB<sub>2</sub> by thermal CVD from Hf[BH<sub>4</sub>]<sub>4</sub> and report the film growth kinetics, microstructure, and composition as a function of the substrate temperature and precursor flux. We also test the performance of 12 nm thick amorphous HfB<sub>2</sub> films as diffusion barriers to separate copper from silicon.

## II. EXPERIMENT

HfB<sub>2</sub> thin films were deposited in a turbopumped chamber of UHV construction that has a base pressure of  $5 \times 10^{-9}$  Torr, most of which is hydrogen.<sup>28</sup> The precursor Hf[BH<sub>4</sub>]<sub>4</sub> is solid with a convenient vapor pressure of  $\sim 15$  Torr at 25 °C.<sup>29</sup> The precursor was maintained at  $-5$  °C in a stainless steel container immersed in a liquid bath; the flow was regulated by a needle valve and delivered to the chamber through a 0.6 cm o.d. stainless steel tube aimed at the substrate. The distance between the end of the tube and the substrate was 7 cm, and could be adjusted by substrate translation. The absolute mass flow rate was calibrated as follows. A capacitance manometer attached downstream of the needle valve was used to monitor the pressure drop in the delivery tube. With the chamber valved off (unpumped), the rate of pressure rise in the chamber was determined as a function of the line pressure, and converted to a mass flow rate using the known chamber volume. The mass flow rate was found to be linear in line pressure drop; a throughput of  $\sim 1.6 \times 10^{14}$  molecules/s was calculated for 1 mTorr line pressure. For the present experiments, the precursor pressure in the chamber (not line-of-sight with the delivery tube) ranged from  $10^{-4}$  to  $10^{-3}$  Torr. Highly conductive ( $\rho=0.01$  Ω cm) *n*-type silicon (100) was used as a substrate for film growth. The substrate dimensions were 20 mm  $\times$  12 mm; prior to loading in the chamber, the substrates were degreased in acetone, isopropyl alcohol and deionized water for 10 min each in an ultrasonic bath. In order to measure the sheet resistance of the HfB<sub>2</sub> film using a four point probe, we occasionally used silicon substrates coated by PECVD with 100 nm of silicon dioxide. The substrates were heated by passing dc electrical current through them. An infrared pyrometer was used to measure the surface temperature; the pyrometer had been calibrated in earlier tests using a thermocouple in contact with the substrate. An *in situ* spectroscopic ellipsometer was employed to identify the onset of film growth, which was especially useful at low substrate temperatures.<sup>30–32</sup>

Temperature programmed reaction (TPR) studies were performed to analyze the precursor reaction rate as a function of substrate temperature. TPR was performed in an ion-pumped UHV system (base pressure  $5 \times 10^{-10}$  Torr) which is

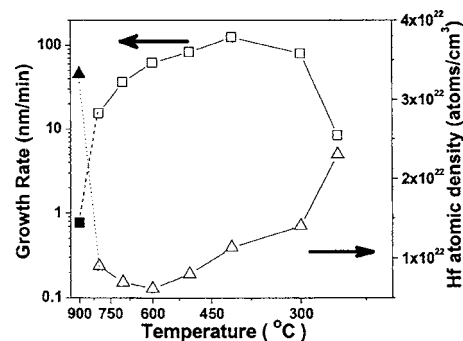


FIG. 1. Log of film growth rate (open squares) and hafnium atomic density from RBS (open triangles) versus inverse absolute temperature. The data from the epitaxial film are indicated by the solid square and solid triangle. The temperature axis is labeled in centigrade for convenience.

connected to the growth system by a transfer tube. The set-up includes a differentially pumped quadrupole mass spectrometer with a 0.4 cm diameter sampling orifice located 5 cm in front of the sample surface. The precursor was introduced through an obliquely-placed delivery tube 5 cm from the sample surface. A rapid temperature ramp rate, 20 °C/s, was used to minimize the temperature rise of surfaces other than the substrate. During the TPR experiments, the chamber pressure did not exceed  $10^{-6}$  Torr.

Film thickness and microstructure were determined by examining the fracture cross-sections in a secondary electron microscope. Film stoichiometry was measured *ex situ* by x-ray photoelectron spectroscopy; the B/Hf atomic ratio was calculated using the handbook instrumental sensitivity factors, which do not account for the loss of boron relative to hafnium at the sample surface during sputter depth profiling. Data were obtained from both the as-grown surface and the bulk, and from multiple areas on each sample. To determine the hafnium atomic density, the area density of hafnium was determined using Rutherford backscattering spectrometry (RBS) and divided by the film thickness measured by SEM. RBS was also used to detect copper diffusion when the films were tested as a diffusion barrier. The film crystallinity was analyzed by x-ray diffraction.

## III. RESULTS AND DISCUSSIONS

### A. Growth kinetics and microstructure

Films were deposited at a precursor pressure (established prior to film growth) of  $1 \times 10^{-4}$  Torr and substrate temperatures of 250–900 °C. The growth rate curve (Fig. 1) appears to show a reaction limited exponential increase at low temperatures followed by a flux limited regime; however the growth rate decreases again at temperatures above 400 °C. The fall in growth rate at high temperatures cannot be explained by an etching reaction because there is no volatile Hf-bearing species except for the precursor itself. Rather, the fall is due to a reduction in the net flux impinging on the substrate, which is the sum of the direct flux from the doser tube and an indirect flux due to the background precursor pressure in the chamber. At high substrate temperatures, the

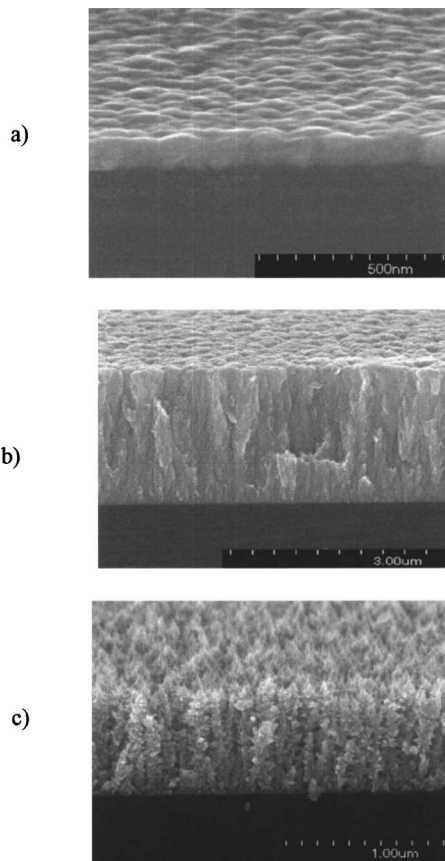


FIG. 2. SEM fracture cross sections of the HfB<sub>2</sub> films on silicon substrates deposited at (a) 250 °C; (b) 400 °C; (c) 700 °C.

sample manipulator and other surfaces inside the chamber are heated radiatively. These surfaces need to attain a temperature of only  $\sim 200$  °C before film starts growing on them, which lowers the precursor partial pressure in the chamber. This is the reason that growth rate decreases at high temperatures. These observations led us to establish a fast ramp rate for TPR experiments, as noted above.

The hafnium atomic density as a function of growth temperature (Fig. 1) shows a drop of  $\sim 70\%$  for intermediate temperatures; therefore the macroscopic growth rate overestimates the quantity of material being deposited and should not be used as a measure of growth kinetics. Figure 1 also shows the hafnium density in an epitaxial HfB<sub>2</sub> film that was deposited at a very low rate ( $< 0.5$  nm/min) on Si (111) at 900 °C, which matches the value ( $3.3 \times 10^{22}$  cm<sup>-3</sup>) calculated from the lattice constants. Our epitaxial growth of (0001) HfB<sub>2</sub> on Si (111) [Fig. 3] is very similar to the result observed by Tolle *et al.* for the growth of ZrB<sub>2</sub> on Si (111) using Zr[BH<sub>4</sub>]<sub>4</sub>.<sup>9</sup> The evidence for epitaxial growth was obtained by x-ray rocking curve measurements; the (0001) rocking curve for the epitaxial HfB<sub>2</sub> film on Si (111) had a FWHM of 0.4°. Detailed investigations of the crystalline texture and epitaxy of HfB<sub>2</sub> films on Si are reported in a separate work.<sup>33</sup>

The microstructures of films grown at 250 and 400 °C [Figs. 2(a) and 2(b)] are strikingly different. The low tem-

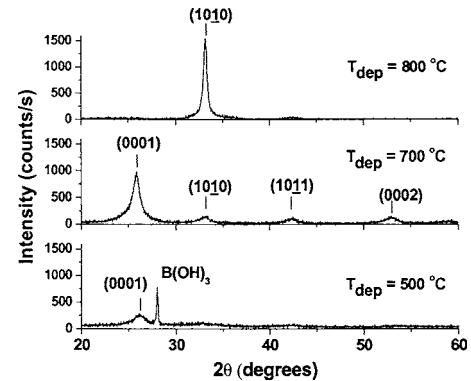


FIG. 3. XRD profile of HfB<sub>2</sub> at different deposition temperatures. Boric acid, B(OH)<sub>3</sub> crystals form when surface boron oxide adsorbs moisture.

perature film is dense and smooth, but the one obtained at higher temperature is columnar and rough. X-ray diffraction confirmed the amorphous nature of both these films. Films deposited at 500 °C and above are crystalline and highly textured [Fig. 3]. The x-ray diffraction spectrum shows one strong peak corresponding to the preferred orientation of the film—(0001) at growth temperatures below 700 °C and (1010) at 800 °C. The films have a faceted columnar microstructure full of voids along the column; this result is consistent with the low Hf atomic density observed by RBS [Fig. 1]. The deposition temperatures are very low compared with the melting point of HfB<sub>2</sub> ( $T/T_m = 0.13-0.3$ ). It is therefore not surprising that at these temperatures we deposit either amorphous or low density crystalline films, the latter being the result of limited surface diffusion.<sup>34,35</sup>

## B. Temperature programmed reaction

TPR experiments provide quantitative data concerning the growth kinetics. The mass spectrum of the precursor (Fig. 4) consists of three envelopes corresponding to BH<sub>y</sub> ( $y=1-3$ ), B<sub>2</sub>H<sub>y</sub> ( $y=1-6$ ), and HfB<sub>x</sub>H<sub>y</sub> ( $x=1-4$ ) fragments. Here the BH<sub>y</sub> and B<sub>2</sub>H<sub>y</sub> intensities arise from precursor decomposition in the mass spectrometer. During film deposition the precursor intensity falls, but these species will be generated as reaction by-products; note that the cracking of B<sub>2</sub>H<sub>6</sub> will also produce BH<sub>y</sub>. Thus the change in BH<sub>y</sub> and B<sub>2</sub>H<sub>y</sub> inten-

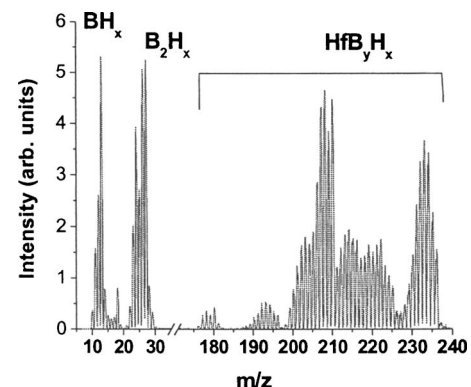


FIG. 4. Precursor cracking pattern in the mass spectrometer.

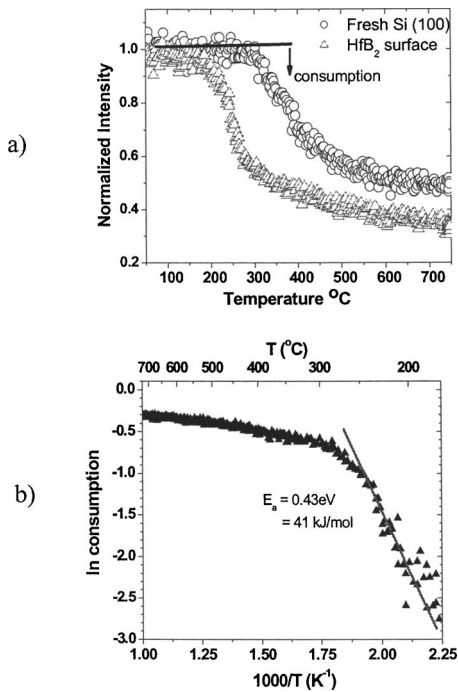


FIG. 5. Precursor intensity variation at  $m/z=208$  during TPR experiments: (a) precursor intensity versus substrate temperature; (b) natural logarithm of precursor consumed versus inverse absolute temperature.

sities is the difference between precursor decomposition and surface generation rates. In contrast, the fall in the  $\text{HfB}_x\text{H}_y$  intensity is directly proportional to the rate of the growth reactions.

In our TPR studies, the silicon substrate was ramped from room temperature to 800 °C at a rate of 20 °C/s as its surface as continually dosed with the precursor. The precursor mass peak at  $m/z=208$  was monitored during the ramp process. Above a threshold temperature, the  $\text{HfB}_x\text{H}_y$  intensity decreases due to consumption of the precursor by growth reactions [Fig. 5(a)]. The intensity reduction, i.e., the precursor consumption rate, consists of an Arrhenius reaction-rate-limited regime with an apparent activation energy of 0.43 eV (41 kJ/mol) and a reactant-flux-limited regime [Fig. 5(b)]. The low activation energy is consistent with the low reaction onset temperature of  $\sim 190$  °C [Fig. 5(a)]. Note that, for this flux, a temperature of only 400 °C is sufficient to saturate the reaction rate.

The reaction onset temperature for a clean Si surface (dipped in 10% HF solution to remove the native oxide) is 100 °C higher than for a surface coated with  $\text{HfB}_2$  in previous TPR ramps [Fig. 5(a)]. We attribute the delayed onset to a nucleation barrier on Si. Supporting evidence was obtained using the in-situ ellipsometer to detect the onset of film growth at fluxes similar to the TPR experiments ( $\sim 10^{-5}$  Torr); for a substrate temperature of  $\sim 300$  °C, a time delay of a few minutes was observed for the formation of any film on Si; but for a temperatures of  $\leq 250$  °C, no film growth was detected during the observation period of 30 min. An even larger barrier was observed on a clean  $\text{SiO}_2$  surface: a higher temperature or flux was needed to observe

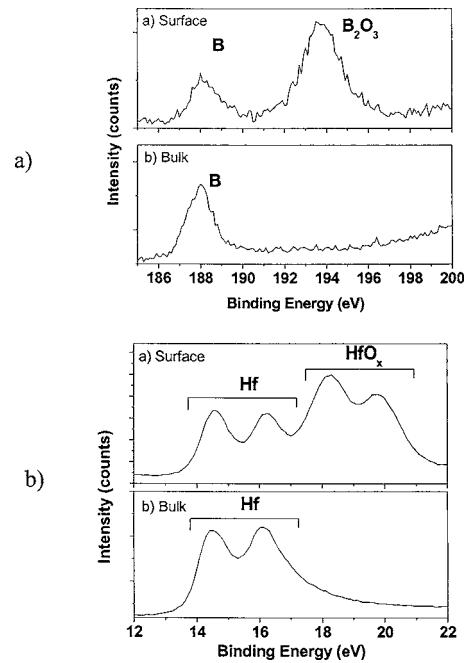


FIG. 6. (a) Boron  $2p$  peak in the XPS; (b) Hf  $5p_{3/2}$  peak in the XPS. The top panel in both the figures is the signal from the surface and the bottom panel is the signal from the bulk. The surface signal contains contributions from both the hafnium boride and the respective oxide phases.

the onset of film growth. The existence of a nucleation barrier has been observed in related systems such as tungsten CVD from the precursor  $\text{WF}_6$ .<sup>36–38</sup>

### C. Film stoichiometry

XPS reveals the presence of boron oxide [Fig. 6(a)] and hafnium oxide [Fig. 6(b)] at the film surface.<sup>39</sup> Oxide formation is unavoidable because the samples are transported in air from the growth system to the XPS chamber. Upon sputter profiling, the oxygen signal rapidly drops below the instrumental detection limit for the films grown at 300 °C and lower. However, the films grown at 400–600 °C contain bulk oxygen. We attribute this finding to the presence of interconnected pores, which allow oxidation of the column boundaries throughout the film thickness. The bulk B/Hf atomic ratio calculated using handbook instrumental sensitivity factors appears to be less than 2 (Fig. 7); this result is an artifact of the preferential sputtering of boron with respect to hafnium during the depth profiling. The apparent B/Hf atomic ratio in the epitaxial  $\text{HfB}_2$  film deposited at 900 °C is similar at 1.3. The epitaxial film has a high degree of crystalline perfection, as evidenced by the sharp XRD peaks, and  $\text{HfB}_2$  has a narrow equilibrium phase width; therefore, the epitaxial film should be essentially stoichiometric. Scatter in the film stoichiometry data is within the instrumental resolution, as confirmed by statistical analysis (single factor analysis of variance,  $\alpha=0.05$ ).<sup>40</sup> Together, these facts indicate that all the films are close to the ideal stoichiometry of B/Hf=2.

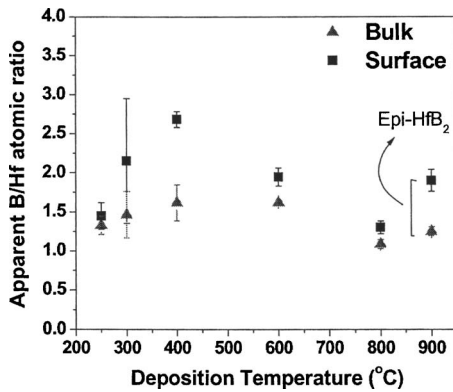


FIG. 7. Apparent B/Hf atomic ratio in the film surface (squares) and bulk (triangles) from XPS. The data points at 900 °C represent the epitaxial film.

#### D. Resistivity and copper diffusion barrier

The room temperature resistivity is  $440 \mu\Omega \text{ cm}$  for  $\text{HfB}_2$  films deposited at 300 °C. At deposition temperatures above 350 °C the resistivity increases sharply as a result of the development of columnar microstructure and the fall in film density. For advanced microelectronic applications, where the growth temperatures should remain below 400 °C the CVD process yields suitable films (Fig. 8).

To test the performance of our  $\text{HfB}_2$  films as impurity diffusion barriers, a 12 nm film was deposited at 250 °C on a planar silicon substrate (the native oxide was removed using 10% HF solution) at a precursor pressure of  $2 \times 10^{-4}$  Torr. This film was coated with 30 nm of copper film in a bell jar evaporator. Two pieces were cleaved from the substrate and annealed for 30 min in vacuum at 600 °C and 700 °C, respectively. RBS of the film annealed at 600 °C showed no mixing of copper and silicon and was identical to the spectrum of the unannealed sample. After the sample had been annealed at 700 °C, however, interdiffusion did occur (Fig. 9). X-ray diffraction of this sample showed  $\text{Cu}_3\text{Si}$  peaks and a diffuse peak from  $(10\bar{1}0)\text{HfB}_2$ . Grain boundary diffusion is hence a possible failure mechanism.

RBS studies of films grown under the same conditions showed that the Hf atomic density was  $\sim 2.3 \times 10^{22} \text{ cm}^{-3}$ .

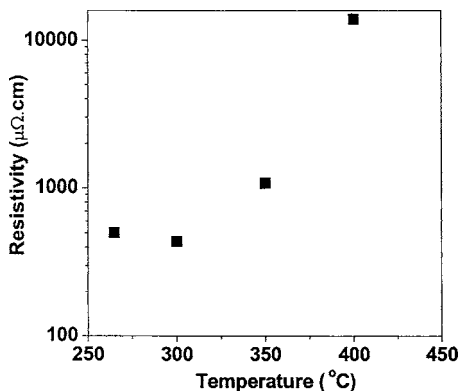


FIG. 8. Film resistivity from four point probe measurements plotted versus deposition temperature.

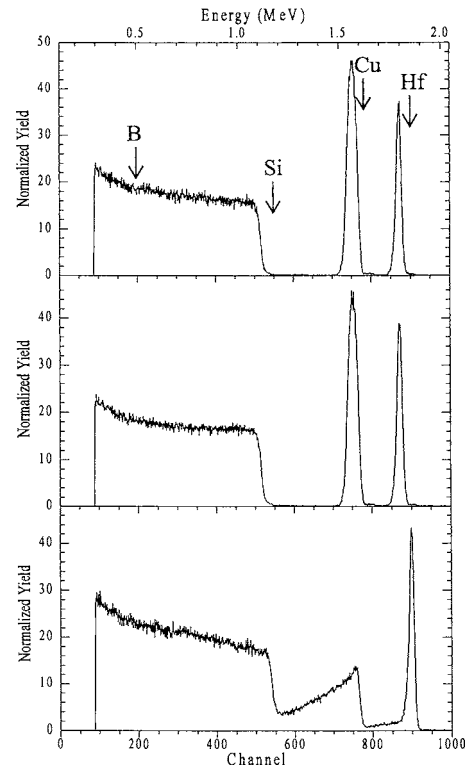


FIG. 9. RBS from a multilayer sample (30 nm)Cu/(12 nm)HfB<sub>2</sub>/Si, as-deposited (top), vacuum-annealed at 600 °C for 30 min (middle) and vacuum annealed at 700 °C for 30 min (bottom).

Although this is only  $\sim 70\%$  of the theoretical value for a single crystal,  $3.3 \times 10^{22} \text{ cm}^{-3}$ , the diffusion barrier still performs well.

#### E. Conformal coverage

CVD can produce highly conformal coatings over nonplanar substrates if the surface reaction probability of the precursor is well below unity.<sup>41,42</sup> Conformal coverage is required for the metallization of trenches and via holes in microelectronic applications, and future generation technologies will involve very high aspect ratio (deep and narrow) features. The reaction limited regime of our CVD process occurs at  $T_{\text{sub}} < 300$  °C; this corresponds to a surface reaction probability less than unity. The reaction probability will also diminish with increasing precursor flux if surface adsorption sites become blocked by chemisorbed fragments of the molecule (analogous to a Langmuir adsorption isotherm). Here, there is a distinct possibility of site blocking by  $\text{BH}_x$  groups from the bulky  $\text{Hf}[\text{BH}_4]_4$  molecule. A combination of low substrate temperature and high precursor flux thus yields a very low surface reaction probability and excellent conformal coverage.

Highly conformal films of  $\text{HfB}_2$  resulted from a deposition temperature of 200 °C and a precursor pressure in the chamber of 1 mTorr [Fig. 10(a)]. On a trench in  $\text{SiO}_2$  that is 170 nm wide and 290 nm deep, the film thickness on the

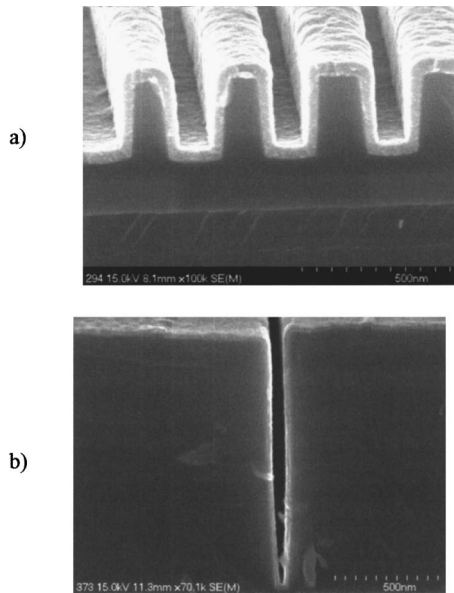


FIG. 10. Conformal nature of the growth process (a) 2.5:1 depth-width aspect ratio trench features coated at 200 °C; (b) 19:1 aspect ratio trench coated at the reaction onset temperature <200 °C.

lower sidewalls is 85% of the thickness on the top. To coat a more demanding feature, a trench which is 65 nm wide and 1200 nm deep (an aspect ratio of 19:1), we increased the precursor pressure to 80 mTorr and slowly increased the temperature to <200 °C until the onset of the growth reaction was just detectable by ellipsometry. (This surface temperature was below the lower limit measurable by our pyrometer.) The film thickness on the lower sidewalls is nearly 100% of the thickness on the top [Fig. 10(b)]. This result is competitive with the conformal coverage afforded by atomic layer deposition (ALD).<sup>43</sup> The CVD growth rate was 0.7 nm/min. An even higher growth rate can be achieved if the aspect ratio of the feature is not very large; for the trench shown in Fig. 10(a), the growth rate was 2.7 nm/min.

#### IV. CONCLUSIONS

A simple CVD route to deposit stoichiometric HfB<sub>2</sub> films at low temperatures is demonstrated. Low temperature films are dense, amorphous, and highly metallic while those deposited at higher temperatures ( $\geq 500$  °C) are crystalline and columnar. Highly conformal films can be obtained by growing the films in a reaction-limited regime, especially at a temperature close to the reaction onset ( $\sim 200$  °C). A 12 nm thick film of amorphous HfB<sub>2</sub> performed well as a diffusion barrier, preventing copper and silicon from intermixing when annealed at 600 °C for 30 min.

#### ACKNOWLEDGMENTS

The authors are grateful to the National Science Foundation for support of this research under Grant Nos. NSF CH-00-76061, NSF DMR-03-54060, and NSF DMR-03-15428.

Compositional and structural analyses of the films were carried out in the Center for Microanalysis of Materials, University of Illinois, which is partially supported by the U.S. Department of Energy under Grant No. DEFG02-91-ER45439.

<sup>1</sup>R. Kieffer and F. Benesovsky, *Hartstoffe* (Springer, Wien, 1963).

<sup>2</sup>*CRC Materials Science and Engineering Handbook*, 2nd ed. (CRC Press, Boca Raton, 1994).

<sup>3</sup>J. W. Sung, D. M. Goedde, G. S. Girolami, and J. R. Abelson, *J. Appl. Phys.* **91**, 3904 (2002).

<sup>4</sup>L. M. Williams, *J. Electrochem. Soc.* **133**, C225 (1986).

<sup>5</sup>J. S. Chen and J. L. Wang, *J. Electrochem. Soc.* **147**, 1940 (2000).

<sup>6</sup>S. T. Lin, Y. L. Kuo, and C. Lee, *Appl. Surf. Sci.* **220**, 349 (2003).

<sup>7</sup>J. Castaing and P. Costa, *Boron and Refractory Borides*, edited by V. I. Matkovich (Springer, New York, 1977), Chap. C.IX, p. 390.

<sup>8</sup>J. Tolle, J. Kouvetakis, D. W. Kim, S. Mahajan, A. Bell, F. A. Ponce, I. S. T. Tsong, M. L. Kottke, and Z. H. D. Chen, *Appl. Phys. Lett.* **84**, 3510 (2004).

<sup>9</sup>J. Tolle, R. Roucka, I. S. T. Tsong, C. Ritter, P. A. Crozier, A. V. G. Chizmeshya, and J. Kouvetakis, *Appl. Phys. Lett.* **82**, 2398 (2003).

<sup>10</sup>C. W. Hu, A. V. G. Chizmeshya, J. Tolle, J. Kouvetakis, and I. S. T. Tsong, *J. Cryst. Growth* **267**, 554 (2004).

<sup>11</sup>C. Y. Tay, I. R. Harris, and S. J. Wright, *J. Electron. Mater.* **18**, 511 (1989).

<sup>12</sup>T. Shikama, Y. Sakai, M. Fukutomi, and M. Okada, *Thin Solid Films* **156**, 287 (1988).

<sup>13</sup>*Binary Alloy Phase Diagrams*, edited by T. B. Massalski, H. Okamoto, P. R. Subramanian, and L. Kacprzak (ASM International, Ohio, 1990).

<sup>14</sup>K. L. Dahm, L. R. Jordan, J. Haase, and P. A. Dearnley, *Surf. Coat. Technol.* **109**, 413 (1998).

<sup>15</sup>E. Kelesoglu, C. Mitterer, M. K. Kazmanli, and M. Urgen, *Surf. Coat. Technol.* **119**, 133 (1999).

<sup>16</sup>O. Knotek, E. Lugscheider, C. Barimani, and M. Moller, *J. Solid State Chem.* **133**, 117 (1997).

<sup>17</sup>M. L. Wu, X. W. Lin, V. P. Dravid, Y. W. Chung, M. S. Wong, and W. D. Sproul, *Tribol. Lett.* **5**, 131 (1998).

<sup>18</sup>C. Mitterer, *J. Solid State Chem.* **133**, 279 (1997).

<sup>19</sup>D. S. Wu, M. L. Lee, T. Y. Lin, and R. H. Horng, *Mater. Chem. Phys.* **45**, 163 (1996).

<sup>20</sup>H. O. Pierson and A. W. Mullendore, *Thin Solid Films* **95**, 99 (1982).

<sup>21</sup>M. Mukaida, T. Goto, and T. Hirai, *J. Mater. Sci.* **26**, 6613 (1991).

<sup>22</sup>B. N. Beckloff and W. J. Lackey, *J. Am. Ceram. Soc.* **82**, 503 (1999).

<sup>23</sup>A. J. Caputo, W. J. Lackey, I. G. Wright, and P. Angelini, *J. Electrochem. Soc.* **132**, 2274 (1985).

<sup>24</sup>S. Veprek, P. Nesladek, A. Niederhofer, F. Glatz, M. Jilek, and M. Sima, *Surf. Coat. Technol.* **109**, 138 (1998).

<sup>25</sup>J. A. Jensen, J. E. Gozum, D. M. Pollina, and G. S. Girolami, *J. Am. Chem. Soc.* **110**, 1643 (1988).

<sup>26</sup>A. L. Wayda, L. F. Schneemeyer, and R. L. Opila, *Appl. Phys. Lett.* **53**, 361 (1988).

<sup>27</sup>S. Reich, H. Suhr, K. Hanko, and L. Szepes, *Adv. Mater. (Weinheim, Ger.)* **4**, 650 (1992).

<sup>28</sup><http://www.mse.uiuc.edu/faculty/abelson.html>

<sup>29</sup>H. R. Hoekstra and J. J. Katz, *J. Am. Chem. Soc.* **71**, 2488 (1949).

<sup>30</sup>J. Humlicek, A. Nebojsa, J. Hora, M. Strasky, J. Spousta, and T. Sikola, *Thin Solid Films* **332**, 25 (1998).

<sup>31</sup>S. Logothetidis, I. Alexandrou, and A. Papadopoulos, *J. Appl. Phys.* **77**, 1043 (1995).

<sup>32</sup>R. W. Collins, I. An, H. Fujiwara, J. C. Lee, Y. W. Lu, J. Y. Koh, and P. I. Rovira, *Thin Solid Films* **313**, 18 (1998).

<sup>33</sup>Y. Yang, S. Jayaraman, D. Y. Kim, G. S. Girolami, and J. R. Abelson, *J. Cryst. Growth* (submitted).

<sup>34</sup>J. A. Thornton, *J. Vac. Sci. Technol.* **6**, 355 (1974).

<sup>35</sup>B. A. Movchan and A. V. Demchisin, *Phys. Met. Metallogr.* **28**, 83 (1969).

<sup>36</sup>K. C. Saraswat, S. Swirhun, and J. P. Mcvittie, *J. Electrochem. Soc.* **131**, C86 (1984).

- <sup>37</sup>U. Jansson and J. O. Carlsson, *Mater. Sci. Eng., B* **17**, 131 (1993).
- <sup>38</sup>T. B. Gorczyca, L. R. Douglas, B. Gorowitz, and R. H. Wilson, *J. Electrochem. Soc.* **136**, 2765 (1989).
- <sup>39</sup>M. Belyansky and M. Trenary, *J. Vac. Sci. Technol. A* **15**, 3065 (1997).
- <sup>40</sup>R. E. DeVor, T. Chang, and J. W. Sutherland, *Statistical Quality Design and Control—Contemporary Concepts and Methods* (Prentice-Hall, New Jersey, 1992).
- <sup>41</sup>H. C. Wulu, K. C. Saraswat, and J. P. Mcvittie, *J. Electrochem. Soc.* **138**, 1831 (1991).
- <sup>42</sup>A. Nuruddin, J. R. Doyle, and J. R. Abelson, *J. Appl. Phys.* **76**, 3123 (1994).
- <sup>43</sup>J. E. Crowell, *J. Vac. Sci. Technol. A* **21**, S88 (2003).